Structure and Assembly of Designed β-Hairpin Peptides in Crystals as Models for β-Sheet Aggregation † , ‡

ARTICLE *in* BIOCHEMISTRY · MARCH 2004

Impact Factor: 3.02 · DOI: 10.1021/bi035522g · Source: PubMed

5 AUTHORS, INCLUDING:

S. Aravinda

36 PUBLICATIONS **763** CITATIONS

SEE PROFILE

Vidya Harini Veldore

HCG-Bangalore Institute of Oncology

15 PUBLICATIONS **128** CITATIONS

SEE PROFILE

Padmanabhan Balaram

Indian Institute of Science

506 PUBLICATIONS **13,956** CITATIONS

SEE PROFILE

Structure and Assembly of Designed β-Hairpin Peptides in Crystals as Models for β-Sheet Aggregation[†,‡]

Subrayashastry Aravinda,[§] Veldore Vidya Harini,[§] Narayanaswamy Shamala,*[,§] Chittaranjan Das,[||] and Padmanabhan Balaram*[,||]

Department of Physics and Molecular Biophysics Unit, Indian Institute of Science, Bangalore 560 012, India

Received August 26, 2003; Revised Manuscript Received December 15, 2003

ABSTRACT: *De novo* designed β-hairpin peptides have generally been recalcitrant to crystallization. The crystal structures of four synthetic peptide β-hairpins, Boc-Leu-Val-Val-DPro-Gly-Leu-Phe-Val-OMe (**1**), Boc-Leu-Phe-Val-DPro-Ala-Leu-Phe-Val-OMe (**2**), Boc-Leu-Val-Val-DPro-Aib-Leu-Val-Val-OMe (**3**), and Boc-Met-Leu-Phe-Val-DPro-Ala-Leu-Val-Val-Phe-OMe (**4**), are described. The centrally positioned DPro-Xxx segment promotes prime β-turn formation, thereby nucleating β-hairpin structures. In all four peptides well-defined β-hairpins nucleated by central type II′ DPro-Xxx β-turns have been characterized by X-ray diffraction, providing a view of eight crystallographically independent hairpins. In peptides **1**−**3** three intramolecular cross-strand hydrogen bonds stabilized the observed β-hairpin, with some fraying of the structures at the termini. In peptide **4**, four intramolecular cross-strand hydrogen bonds stabilized the hairpin. Peptides **1**−**4** reveal common features of packing of β-hairpins into crystals. Two-dimensional sheet formation mediated by intermolecular hydrogen bonds formed between antiparallel strands of adjacent molecule is a recurrent theme. The packing of two-dimensional sheets into the crystals is mediated in the third dimension by bridging solvents and interactions of projecting side chains, which are oriented on either face of the sheet. In all cases, solvation of the central DPro-Xxx peptide unit β-turn is observed. The hairpins formed in the octapeptides are significantly buckled as compared to the larger hairpin in peptide **4**, which is much flatter. The crystal structures provide insights into the possible modes of β-sheet packing in regular crystalline arrays, which may provide a starting point for understanding β-sandwich and cross-β-structures in amyloid fibrils.

β-Sheets are widely distributed in protein structures. In globular proteins, multistranded β-sheets are generally buried in protein interiors and are stabilized by networks of interstrand hydrogen bonds (*1*, *2*). In membrane proteins the β-barrel, a closed β-sheet assembly facilitated by the intrinsic curvature of sheets, is a widespread structural feature (*3*). Quite often, antiparallel strands in protein structures are connected by tight turns, generally two-residue β-turns, with registered cross-strand hydrogen bonds orienting the antiparallel segments of the polypeptide chain, resulting in hairpin formation (*4*−*8*). Considerable recent interest in β-sheet structures stems from their occurrence in insoluble polypeptide deposits, which form amyloid-like fibrils (*9*−*11*). Attempts to design β-sheets from "first principles" have focused on β-hairpins as the fundamental unit in generating multistranded structures (*12*−*15*). X-ray diffraction studies of β-hairpin peptides in single crystals can provide invaluable information on the packing and three-dimensional assembly of extended polypeptide strands. We have therefore been investigating the design and construction of β-hairpin peptides with a high propensity to assemble into single crystals.

The use of stereochemically constrained amino acids in the design of conformationally well-defined peptides has attracted attention in recent years. Helical folding in designed sequences has been achieved by the incorporation of α-aminoisobutyric acid (Aib)[1] and related $C^{\alpha,\alpha}$ dialkylated residues (*15*−*17*). The construction of β-hairpin structures has been approached by the incorporation of centrally located DPro-Xxx segments, which stabilize the formation of prime β-turns (type I′/II′), serving as nuclei for the formation of antiparallel β-strands registered by interchain hydrogen bonds (*18*−*24*). The use of DPro-Xxx segments is a consequence of analysis of β-hairpins in protein structures, which revealed that proper registry of antiparallel strands is often realized by nucleating turns favoring type I′/II′ conformations (*4*−*7*). In the DPro residue the torsion angle ϕ is restricted to a value of $+60° \pm 20°$, constraining DPro-Xxx β-turns which incorporate this residue at the $i + 1$ position (*15*). Recent studies from this laboratory have demonstrated the utility of centrally placed DPro-Xxx segments in nucleating isolated β-hairpins (*25*−*29*) and in the generation of multistranded β-sheet structures (*30*−*33*). Crystal structure determination and detailed NMR

[†] This work was supported by a grant from the Council of Scientific and Industrial Research and a program grant in the area of Molecular Diversity and Design by the Department of Biotechnology, Government of India. V.V.H. is a Senior Research Fellow of the Council of Scientific and Industrial Research, Government of India.

[‡] Atomic coordinates have been deposited in the Cambridge Crystallographic Data Centre: CCDC 218047, CCDC 218048, CCDC 218049, and CCDC 218050.

* To whom correspondence should be addressed. N.S.: fax, 91-80-23602602/91-80-23600683; e-mail, shamala@physics.iisc.ernet.in. P.B.: fax, 91-80-23600683/91-80-23600535; e-mail, pb@mbu.iisc.ernet.in.

[§] Department of Physics.

[||] Molecular Biophysics Unit.

[1] Abbreviations: Aib, α-aminoisobutyric acid; DPro, D-proline.

10.1021/bi035522g CCC: $27.50
Published on Web 01/29/2004

Table 1: Crystal and Diffraction Parameters

	peptide **1**	peptide **2**	peptide **3**	peptide **4**
empirical formula	$C_{49}H_{78}N_8O_{11}\cdot H_2O$	$2(C_{54}H_{75}N_8O_{11})\cdot H_2O + C_3H_8O$	$C_{47}H_{84}N_8O_{11}\cdot H_2O +$ DMF	$C_{64}H_{100}N_{10}O_{13}S_1\cdot H_2O$
crystal habit	clear and rectangular	clear and rod	clear and rectangular	clear and cubical
crystal size (mm)	0.25 × 0.2 × 0.07	0.6 × 0.2 × 0.15	0.3 × 0.2 × 0.09	0.6 × 0.6 × 0.4
crystallizing solvent	ethanol/ 2-propanol	2-propanol/water	DMF and CCl_4	methanol/water
space group	$P2_12_12_1$	$P2_12_12_1$	$P1$	$P1$
cell parameters				
a (Å)	9.883(2)	19.107(4)	9.882(4)	12.153(12)
b (Å)	12.2378(10)	23.905(6)	11.288(4)	24.10(2)
c (Å)	46.861(7)	28.45(7)	15.734(6)	27.99 (3)
α (deg)	90.0	90.0	107.545	101.02(5)
β (deg)	90.0	90.0	90.017	102.51(6)
γ (deg)	90.0	90.0	104.261	104.62(3)
volume ($Å^3$)	5667.8(15)	12995(5)	1616.6(11)	7477(13)
Z	4	8	1	4
molecules/asym unit	1	2	1	4
cocrystallized solvent	one water molecule	three waters and one 2-propanol	one water molecule + one DMF	four water molecules
molecular weight	973.21	1072.82	1026.32	1265.6
density (g/cm^3) (cal)	1.141	1.097	1.054	1.124
F(000)	2104	4628	558	2728
radiation	Cu Kα ($\lambda = 1.5418$ Å)	Mo Kα ($\lambda = 0.71073$ Å)	Mo Kα ($\lambda = 0.71073$ Å)	Mo Kα ($\lambda = 0.71073$ Å)
temperature (°C)	21	21	21	21
2*θ* max (deg)	140	53.88	54	50.06
scan type	$\omega - 2\theta$	ω	ω	ω
scan speed	variable			
measured reflections	6804	131671	16737	189392
independent reflections	6227	26093	12068	50361
unique reflections	5996	14340	6327	26309
observed reflections [$\|F\| > 4\sigma(F)$]	2915	9890	4290	22088
final *R* (%)	8.05	8.86	7.78	10.62
final wR_2 (%)	19.25	23.29	20.23	24.94
resolution (Å)	0.82	0.78	0.78	0.84
goodness of fit (S)	1.05	0.857	1.063	0.913
$\Delta\rho_{max}$ (e $Å^{-3}$)	0.31	0.51	0.52	0.44
$\Delta\rho_{min}$ (e $Å^{-3}$)	−0.29	−0.29	−0.23	−0.24
no. of restraints/parameters	2/694	7/1330	3/649	35/3157
data to parameter ratio	4.2:1	7.4:1	6.6:1	6.9:1

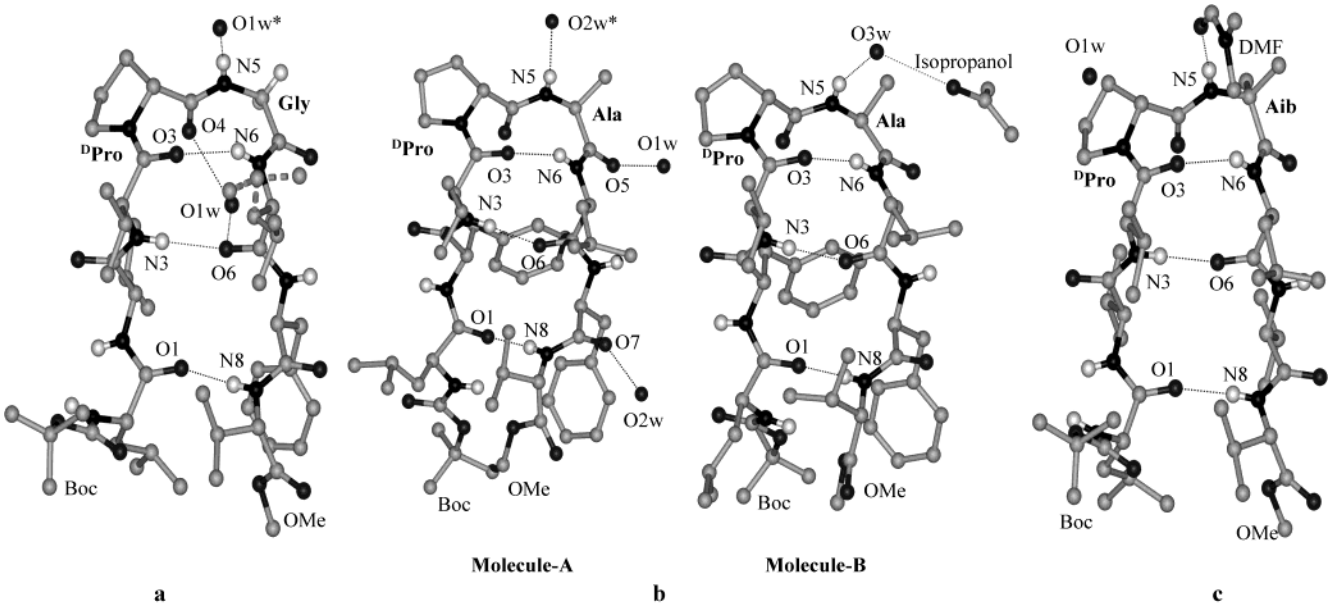

FIGURE 1: Molecular conformation in crystals of peptides **1**−**3**. Hydrogen bonds are shown as dotted lines. (a) Boc-Leu-Val-Val-DPro-Gly-Leu-Phe-Val-OMe (**1**) (O1w* is the symmetry-related water molecule). (b) Boc-Leu-Phe-Val-DPro-Ala-Leu-Phe-Val-OMe (**2**) (O2w* is the symmetry-related water molecule). Two molecules in the asymmetric unit are shown. (c) Boc-Leu-Val-Val-DPro-Aib-Leu-Val-Val-OMe (**3**).

analysis in solution remain the most definitive means of establishing the success of a specific molecular design strategy. In the case of helical peptides a very large body of structural data in crystals has accumulated over the past 25 years, because of the facility with which helices form single crystals suitable for X-ray diffraction. β-Hairpins and designed β-sheets have proved more difficult to crystallize. At present the extent of structural information on designed β-hairpins is relatively limited. We describe in this report the crystal structure determination of four synthetic β-hairpin

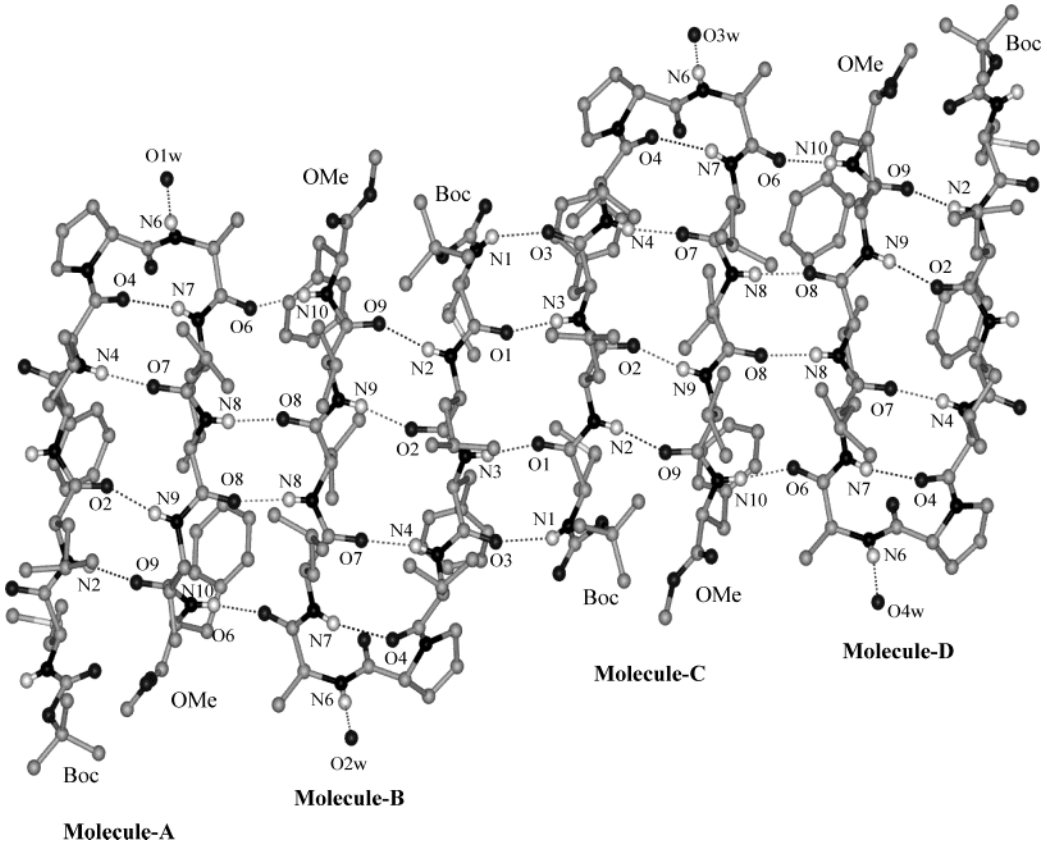

FIGURE 2: Molecular conformation of the decapeptide Boc-Met-Leu-Phe-Val-DPro-Ala-Leu-Val-Val-Phe-OMe (**4**). Four molecules in the asymmetric unit are shown.

Table 2: Torsion Angles (deg) for Peptides **1**−**3**[a]

				peptide **2** (Xxx = Ala)								
	peptide **1** (Xxx = Gly)[b]			molecule A			molecule B			peptide **3** (Xxx = Aib)		
residue	ϕ	ψ	ω	ϕ	ψ	ω	ϕ	ψ	ω	ϕ	ψ	ω
Leu(1)	−107.0[c]	−55.4	178.2	−150.3[c]	131.0	175.9	−121.9[c]	127.3	−173.8	−112.1[c]	−53.6	176.8
Val(2)/Phe(2)	−113.0	118.6	−179.4	−118.9	143.8	171.4	−128.7	138.4	165.5	−116.0	118.4	−173.8
Val(3)	−127.6	88.9	−171.7	−118.2	99.6	−165.5	−108.2	101.2	−167.5	−127.3	81.0	−172.2
DPro(4)	**62.5**	**−132.4**	176.0	**55.9**	**−134.5**	−178.2	**62.4**	**−127.2**	174.6	**59.9**	**−129.3**	179.7
Xxx(5)	**−80.6**	**−3.5**	178.2	**−81.3**	**−4.4**	−177.9	**−97.3**	**5.9**	179.0	**−60.1**	**−30.4**	−169.7
Leu(6)	−81.6	135.6	174.0	−83.7	124.7	171.2	−85.1	122.1	178.9	−81.8	134.1	170.6
Val(7)/Phe(7)	−120.3	116.5	−174.1	−84.4	125.2	−178.9	−87.8	127.2	179.3	−116.3	115.1	−177.5
Val(8)	−77.6	−52.6[d]	−176.6[e]	−97.5	−65.5[d]	−178.9[e]	−123.8	0.0[d]	176.2[e]	−71.7	−37.0[d]	178.8[e]

			peptide **2** (Xxx = Ala)					
	peptide **1** (Xxx = Gly)[b]		molecule A		molecule B		peptide **3** (Xxx = Aib)	
side chain	χ^1	χ^2	χ^1	χ^2	χ^1	χ^2	χ^1	χ^2
Leu(1)	−177.1	66.9, −168.9	−173.1	−162.6, 79.5	−69.8	39.8, −176.9	177.8	59.2, −175.1
Val(2)/Phe(2)	−63.3, 171.1		−74.7	82.7, −96.2	−71.2	83.7, −94.5	−56.2, 179.5	
Val(3)	−51.3, −175.9		179.5, −61.2		−58.1,179.5		−49.2, −173.8	
Leu(6)	−50.7 (139.2)	−76.7, 167.8 (29.7, −103.8)	174.6	−166.0, 66.9	−177.4	70.7, −162.3	172.3	71.5, −166.4
Val(7)/Phe(7)	−175.8	−98.0, 80.0	178.6	74.0, −105.0	−175.9	61.4, −121.6	−56.3, 178.6	
Val(8)	−65.1, 170.9		176.6, −63.4		−58.7, 67.0		−60.3, 171.2	

[a] The torsion angles for rotation about bonds of the peptide backbone (ϕ, ψ, and ω) and about bonds of the amino acid side chains (χ^1, χ^2) are as suggested by the IUPAC−IUB Commission on Biochemical Nomenclature (*55*). [b] The Leu(6) side chain has a disorder occupancy of C6g = 0.6, C6d1 = 0.53, and C6d2 = 0.56. The χ values are given in parantheses. [c] C′(0)−N(1)−C$^\alpha$(1)−C′(1). [d] N(8)−C$^\alpha$(8)−C′(8)−O(OMe). [e] C$^\alpha$(8)−C′(8)−O(OMe)−C(OMe).

peptides, Boc-Leu-Val-Val-DPro-Gly-Leu-Phe-Val-OMe (**1**), Boc-Leu-Phe-Val-DPro-Ala-Leu-Phe-Val-OMe (**2**), Boc-Leu-Val-Val-DPro-Aib-Leu-Val-Val-OMe (**3**), and Boc-Met-Leu-Phe-Val-DPro-Ala-Leu-Val-Val-Phe-OMe (**4**). The choice of the sequences is based on positioning a central DPro-Xxx sequence flanked by tri- or tetrapeptide strands containing largely nonpolar side chains. The incorporation of Phe residues at facing positions on antiparallel strands in peptide **2** was intended to explore the possibility of cross-strand aromatic interactions (*34*−*36*).

Table 3: Torsion Angles (deg) for Peptide **4**

	peptide **4** (Xxx = Ala)											
	molecule A			molecule B			molecule C			molecule D		
residue	ϕ	ψ	ω	ϕ	ψ	ω	ϕ	ψ	ω	ϕ	ψ	ω
Met(1)	−94.8[a]	124.9	−171.9	−77.8[a]	133.6	176.7	−78.3[a]	132.5	177.4	−93.2[a]	124.4	−172.0
Leu(2)	−139.8	137.7	170.9	−118.9	119.9	−178.1	−119.6	118.9	−178.9	−140.2	138.3	171.6
Phe(3)	−123.6	103.5	−171.9	−118.9	103.7	−170.1	−118.8	103.4	−167.6	−124.0	102.9	−172.8
Val(4)	−124.9	75.9	−175.4	−131.2	73.2	174.5	−132.6	73.9	174.7	−123.9	77.3	−176.3
DPro(5)	**59.8**	**−123.3**	−179.8	**73.2**	**−118.1**	176.6	**72.1**	**−117.1**	178.1	**60.6**	**−122.9**	179.5
Xxx(6)	**−69.8**	**−15.2**	−176.4	**−74.1**	**−14.5**	−177.5	**−74.8**	**−15.1**	−177.5	**−74.0**	**−8.4**	−178.8
Leu(7)	−96.3	126.1	177.3	−105.4	132.6	172.3	−105.6	129.8	171.8	−99.6	125.0	178.4
Val(8)	−131.6	129.8	168.9	−132.6	129.0	177.5	−130.7	129.3	177.1	−130.6	129.3	167.2
Val(9)	−117.7	116.7	−179.1	−120.8	121.3	−174.8	−120.2	119.7	−176.8	−114.0	119.2	−178.8
Phe(10)	−82.2	−177.4[b]	−159.8[c]	−95.5	158.1[b]	177.4[c]	−92.6	158.3[b]	−178.3[c]	−91.5	172.5[b]	−170.4[c]

	peptide **4** (Xxx = Ala)							
	molecule A		molecule B		molecule C		molecule D	
side chain	χ^1	χ^2	χ^1	χ^2	χ^1	χ^2	χ^1	χ^2
Met(1)[d]	177.0	169.1	178.1	174.3	178.9	172.2	−179.2	171.3
Leu(2)	−42.3	−71.2, 160.4	−176.6	69.5, −172.5	−174.9	70.2, −167.8	−37.8	−79.4, 161.5
Phe(3)	−67.2	76.6, −103.1	176.4	59.9, −118.6	175.5	61.9, −121.2	−68.0	74.9, −104.4
Val(4)	−54.8, −179.5		−66.3, 53.7		−67.0, 48.6		−55.8, −177.2	
Leu(7)	−64.1	−107.3, 107.6	172.3	61.9, −177.0	170.7	65.3, −173.6	−60.6	−115.9, 114.5
Val(8)	−54.0, 179.7		−34.2, −167.4		−38.9, −165.9		−52.2, −173.9	
Val(9)	−55.2, 173.6		−49.9, −170.8		−53.0, −171.8		−49.7, 177.6	
Phe(10)	−66.4	−76.5, 96.8	−64.4	−81.7, 99.4	−62.1	−82.7, 98.0	−79.7	−62.8, 107.5

[a] C′(0)−N(1)−C$^\alpha$(1)−C′(1). [b] N(10)−C$^\alpha$(10)−C′(10)−O(OMe). [c] C$^\alpha$(10)−C′(10)−O(OMe)−C(OMe). [d] χ^3 for Met (1) = 80.1, 121.3, 95.2, and 76.4 for molecules A, B, C, and D, respectively.

EXPERIMENTAL PROCEDURES

Peptide Synthesis. Peptides **1**−**4** were synthesized by conventional solution-phase methods using a fragment condensation strategy. The *tert*-butyloxycarbonyl (Boc) group was used for N-terminus, and the C-terminus was protected as a methyl ester. Deprotections were performed using 98% formic acid and saponification for the N- and C-terminal protection groups, respectively. Couplings were mediated by dicyclohexylcarbodiimide/1-hydroxybenzotriazole (DCC/HOBT). All of the intermediates were characterized by ^{1}H NMR (80 MHz) and TLC (silica gel, 9:1 chloroform/methanol) and were used without further purification. The final peptides were purified by medium-pressure liquid chromatography (MPLC) on a C_{18} column (40−60 μm) followed by HPLC (C_{18}, 5−10 μm), employing methanol/water gradients. The homogeneity of the purified peptides was ascertained by analytical HPLC. The purified peptides were characterized by electospray and MALDI mass spectrometry and by complete assignment of the 500 MHz NMR spectra (M_{cal} = 957.6, M_{obs} = 979.7 [M + Na$^+$] for peptide **1**; M_{cal} = 1018.5, M_{obs} = 1041.7 [M + Na$^+$] for peptide **2**; M_{cal} = 936.0, M_{obs} = 959.7 [M + Na$^+$] for peptide **3**; M_{cal} = 1249.6, M_{obs} = 1273.0 [M + Na$^+$] for peptide **4**).

X-ray Diffraction. Single crystals of peptides **1**−**4** were grown from ethanol/2-propanol, 2-propanol/water, dimethylformamide/carbon tetrachloride, and methanol/water solutions, respectively. X-ray diffraction data were collected on a CAD4 diffractometer (Cu Kα) for peptide **1** and on a Bruker AXS SMART APEX CCD diffractometer (Mo Kα) for peptides **2**−**4**. Crystal and diffraction data and refinement details are summarized in Table 1.

*Boc-Leu-Val-Val-*D*Pro-Gly-Leu-Phe-Val-OMe (1).* The structure was solved by direct methods using SHELXS-97 (*37*). This gave a fragment containing 62 atoms. The remaining atoms and a cocrystallized water molecule were located from difference Fourier maps. Full-matrix least-squares refinement was carried out using SHELXL-97 (*38*). The hydrogen atoms were fixed geometrically in idealized positions and refined in the final cycle of refinement as riding over the atoms to which they are bonded. The final *R*-factor was 8.05%.

*Boc-Leu-Phe-Val-*D*Pro-Ala-Leu-Phe-Val-OMe (2), Boc-Leu-Val-Val-*D*Pro-Aib-Leu-Val-Val-OMe (3), and Boc-Met-Leu-Phe-Val-*D*Pro-Ala-Leu-Val-Val-Phe-OMe (4).* The structures were solved by direct methods using SHELXD (*39*). For peptide **2**, two fragments were obtained containing 66 and 60 atoms. For peptide **3**, a fragment containing 55 atoms was obtained. The crystal structure of peptide **4** contains 356 non-hydrogen atoms in the asymmetric unit. Despite this size, structure solution using direct methods proceeded smoothly. Four fragments were obtained containing 67, 65, 58, and 54 atoms. The remaining atoms and solvent molecules were located from difference Fourier maps. Full-matrix least-squares refinement was carried out using SHELXL-97. The hydrogen atoms were fixed geometrically in the idealized positions and refined in the final cycle of refinement as riding over the atoms to which they are bonded. The final *R*-factor was 8.86% for peptide **2**, 7.78% for peptide **3**, and 10.62% for peptide **4**.

RESULTS

Structures of β-Hairpins. Crystals of peptides **1** and **3** contain one molecule in the asymmetric unit. Peptide **2** crystallizes with two molecules in the asymmetric unit, while peptide **4** reveals the presence of as many as four molecules in the asymmetric unit. The structure determinations, therefore, provide a view of as many as eight independent

Table 4: Hydrogen Bonds in Peptides **1**−**3**

type	donor	acceptor	N···O/O···O (Å)	H···O (Å)	C═O···H (deg)	C═O···N (deg)	O···H−N (deg)
			Peptide **1**				
intermolecular	N(1)	O(7)[a]	2.948	2.139	145.1	150.9	156.6
intermolecular	N(2)	O(7)[a]	3.058	2.210	148.7	151.3	168.5
intermolecular	N(7)[a]	O(2)	3.053	2.218	141.7	146.2	163.8
peptide−water	N(5)[b]	O1w	2.820	1.980			165.1
solvent−peptide	O1W	O(4)	2.744				
solvent−peptide	O1W	O(6)	2.871				
intramolecular	N(3)	O(6)	3.073	2.216	147.1	148.3	175.1
intramolecular	N(6)	O(3)	2.982	2.191	135.6	133.1	152.8
intramolecular	N(8)	O(1)	2.910	2.051	151.9	152.8	176.7
			Peptide **2**				
intermolecular	N(2)A	O(2)B	2.856	2.005	151.4	154.4	170.1
peptide−water	N(5)A[c]	O2w	2.918	2.096			159.6
intermolecular	N(7)A	O(7)B[d]	2.951	2.095	165.9	164.2	173.7
intermolecular	N(2)B	O(2)A	2.872	2.068	151.7	156.9	155.5
peptide−water	N(5)B	O3w	3.047	2.235			157.2
peptide−water	N(7)B[d]	O1w	2.927	2.067			177.1
solvent−peptide	O1w	O(5)A	2.713				
solvent−peptide	O2w	O(7)A	2.799				
solvent−peptide	O2w	O(8)B[d]	3.052				
solvent−peptide	O3w	O(8)B[e]	3.387				
solvent−solvent	O3w	O(P)[f]	2.834				
molecule A							
intramolecular	N(3)	O(6)	2.858	2.011	152.5	154.5	168.0
intramolecular	N(6)	O(3)	3.001	2.206	133.5	130.9	153.8
intramolecular	N(8)	O(1)	2.924	2.066	162.6	162.8	175.2
molecule B							
intramolecular	N(3)	O(6)	2.904	2.079	154.0	154.5	160.5
intramolecular	N(6)	O(3)	2.970	2.154	135.5	134.3	158.3
intramolecular	N(8)	O(1)	2.929	2.070	157.1	157.9	177.1
			Peptide **3**				
intermolecular	N(1)	O(7)[a]	2.879	2.049	148.8	152.5	161.8
intermolecular	N(2)	O(7)[a]	3.128	2.292	147.3	150.8	163.9
intermolecular	N(7)	O(2)[d]	3.037	2.189	152.0	154.6	168.7
peptide−solvent	N(5)	O(S)[g]	2.938	2.081	148.7	148.6	174.3
intramolecular	N(3)	O(6)	2.883	2.023	157.9	157.7	177.7
intramolecular	N(6)	O(3)	3.030	2.246	132.4	126.9	151.5
intramolecular	N(8)	O(1)	2.886	2.035	153.4	155.0	169.8

[a] Symmetry related by $x + 1, y, z$. [b] Symmetry related by $-x, y + {}^1/_2, -z + {}^3/_2$. [c] Symmetry related by $-x, y - {}^1/_2, {}^1/_2 - z$. [d] Symmetry related by $x - 1, y, z$. [e] Symmetry related by ${}^3/_2 - x, -y, z + {}^1/_2$. [f] O(P) is the oxygen of the 2-propanol molecule. [g] O(S) is the oxygen atom of the DMF molecule.

β-hairpin molecules. The molecular conformations of peptides **1**−**4** in crystals are shown in Figures 1 and 2. It is evident, in all cases, that β-hairpin conformations registered with at least three intramolecular hydrogen bonds are observed. The backbone and side chain torsion angles are given in Tables 2 and 3, and the relevant hydrogen bond parameters are listed in Tables 4 and 5. In peptide **1** the Leu(6) side chain is disordered with a occupancy of C6g = 0.6/0.4, C6d1 = 0.53/0.47, and C6d2 = 0.56/0.44 over two positions. In all cases, the DPro-Xxx segment adopts a type II′ β-turn conformation (torsion angles for an idealized type II′ β-turn are $\phi_{i+1} = 60°$, $\psi_{i+1} = -120°$, $\phi_{i+2} = -80°$, $\psi_{i+2} = 0°$) (*40*). Interestingly, of the 11 available β-hairpin structures characterized thus far (including the four examples in the present study) type I′ β-turns have been observed only in three cases: Boc-Leu-Val-β-Phe-Val-DPro-Gly-Leu-β-Phe-Val-Val-OMe (*27*), Boc-Leu-Val-β-Val-DPro-Gly-β-Leu-Val-Val-OMe (*28*), and Boc-Leu-Phe-Val-Aib-DAla-Leu-Phe-Val-OMe (*34*) (ideal values for type I′ β-turns are $\phi_{i+1} = 60°$, $\psi_{i+1} = 30°$, $\phi_{i+2} = 90°$, $\psi_{i+2} = 0°$). Clearly, the DPro-Xxx segment appears to have a high propensity to facilitate type II′ β-turn conformations. Inspection of the torsion angles in Table 2 reveals that in peptides **1**−**3** residues at positions 1, 2, 3, 6, and 7 adopt values anticipated for extended strand segments. However, Val(8) adopts ϕ, ψ values which deviate significantly from the values in strands, resulting in the absence of the cross-strand Leu(1) NH··· OC Val(8) hydrogen bond. In the octapeptide hairpins, an ideal structure would be stabilized by four intramoleclar hydrogen bonds, whereas in peptides **1**−**3,** only three are observed as a result of fraying at the edges of the hairpin. In the decapeptide **4**, all of the four independent hairpins in the asymmetric unit possess the anticipated four intramolecular hydrogen bonds. In hairpins **1** and **2**, there is a pronounced buckling of the sheets when the molecule is viewed in a direction along the intramolecular hydrogen bond. The hairpin is appreciably flatter in peptides **3** and **4** (Figure 3). A comparison of the torsion angles for the type II′ β-turns reveals that the ψ_{Xxx} is appreciably larger in peptide **3** (−30.4°) as compared to the ψ_{Xxx} in peptides **1** and **2**, where the value lies between −3.5° and 5.9°. In the decapeptide **4**, the ψ_{Xxx} values for the four molecules lie between −8.4° and −15.2°. The values of the virtual torsion angle ($C^{\alpha}_{i}-C^{\alpha}_{i+1}-C^{\alpha}_{i+2}-C^{\alpha}_{i+3}$) (*7*), which is a measure of flattening in the β-turn region, are −16.7° for peptide **1**, −21.4° and −27.1° for peptide **2**, −3.4° for peptide **3**, and

Table 5: Hydrogen Bonds in Peptide **4**

type	donor	acceptor	N···O/O···O (Å)	H···O (Å)	C═O···H (deg)	C═O···N (deg)	N—H···O (deg)
intermolecular	N(1)-A	O(3)-D[a]	3.040	2.260	157.4	152.3	150.9
intramolecular	N(2)-A	O(9)-A	2.940	2.110	136.4	141.3	161.9
intermolecular	N(3)-A	O(1)-D[a]	2.818	1.963	165.0	164.3	173.2
intramolecular	N(4)-A	O(7)-A	2.842	1.996	172.7	169.6	167.7
peptide−water	N(6)-A	O1w	2.935	2.085			169.4
intramolecular	N(7)-A	O(4)-A	3.004	2.170	129.7	127.6	163.0
intermolecular	N(8)-A	O(8)-B	2.900	2.081	164.7	169.1	158.8
intramolecular	N(9)-A	O(2)-A	2.879	2.043	145.2	149.7	163.8
intermolecular	N(10)-A	O(6)-B	2.980	2.157	164.3	163.2	160.2
solvent−peptide	O1w	O(5)-D[b]	2.729				
intermolecular	N(1)-B	O(3)-C	2.954	2.194	155.5	146.4	147.2
intramolecular	N(2)-B	O(9)-B	2.913	2.073	149.1	153.2	165.3
intermolecular	N(3)-B	O(1)-C	2.858	2.005	153.1	155.6	171.6
intramolecular	N(4)-B	O(7)-B	2.881	2.040	176.5	173.9	165.5
peptide−water	N(6)-B	O2w	2.900	2.053			168.3
intramolecular	N(7)-B	O(4)-B	3.250	2.415	117.8	116.7	163.9
intermolecular	N(8)-B	O(8)-A	2.911	2.053	164.6	165.2	175.9
intramolecular	N(9)-B	O(2)-B	2.877	2.022	156.5	158.7	172.3
intermolecular	N(10)-B	O(6)-A	2.913	2.062	147.0	149.6	170.3
solvent−peptide	O2w	O(5)-C[c]	2.712				
intermolecular	N(1)-C	O(3)-B	2.992	2.218	154.2	145.9	149.7
intramolecular	N(2)-C	O(9)-C	2.900	2.055	151.0	154.6	167.4
intermolecular	N(3)-C	O(1)-B	2.856	2.003	151.4	154.1	170.9
intramolecular	N(4)-C	O(7)-C	2.883	2.044	175.2	174.1	165.0
peptide−water	N(6)-C	O3w	2.971	2.117			171.5
intramolecular	N(7)-C	O(4)-C	3.271	2.441	118.0	117.0	162.4
intermolecular	N(8)-C	O(8)-D	2.910	2.050	164.1	164.6	178.1
intramolecular	N(9)-C	O(2)-C	2.854	1.999	156.5	158.7	172.3
intermolecular	N(10)-C	O(6)-D	2.882	2.026	147.8	149.0	173.3
solvent−peptide	O3w	O(5)-B[d]	2.744				
intermolecular	N(1)-D	O(3)-A[e]	3.042	2.279	157.2	152.3	148.0
intramolecular	N(2)-D	O(9)-D	2.939	2.109	139.7	144.5	162.1
intermolecular	N(3)-D	O(1)-A[e]	2.830	1.975	163.8	163.3	172.9
intramolecular	N(4)-D	O(7)-D	2.842	1.995	171.6	168.1	168.2
peptide−water	N(6)-D	O4w	2.925	2.074			169.9
intramolecular	N(7)-D	O(4)-D	3.015	2.174	127.6	126.5	165.5
intermolecular	N(8)-D	O(8)-C	2.904	2.076	167.6	170.9	161.3
intramolecular	N(9)-D	O(2)-D	2.869	2.035	144.7	149.2	163.0
intermolecular	N(10)-D	O(6)-C	2.970	2.121	160.3	160.6	169.1
solvent−peptide	O4w	O(5)-A[f]	2.745				

[a] Symmetrically related by $x, y-1, z+1$. [b] Symmetrically related by $x+1, y, z+1$. [c] Symmetrically related by $x, y-1, z$. [d] Symmetrically related by $x+1, y+1, z$. [e] Symmetrically related by $x, y+1, z-1$. [f] Symmetrically related by $x, y, z-1$.

1.1°, 4.7°, 4.9°, and 0.2° for peptide **4**. Notably, the values are close to 0° in the case of peptide **3** and all of the four independent molecules in peptide **4**.

A common feature of all of the hairpin structures determined in this study is the solvation of the central peptide unit of the DPro-Xxx β-turn. In peptide **1**, a water molecule bridges DPro(4) CO and Leu(6) CO within a single hairpin, while the Gly(5) NH is hydrogen bonded to the bound water of a symmetry-related molecule. In peptides **2** and **4**, the Xxx NH group forms a hydrogen bond to a water molecule which bridges symmetry-related hairpins. In peptide **3**, the carbonyl group of a dimethylformamide molecule forms a hydrogen bond to the exposed NH group of the β-turn segment. Interestingly, solvation of the central peptide unit in β-turns appears to be a recurrent feature in proteins (*41*).

Side Chain−Side Chain and Side Chain−Backbone Interactions. The β-hairpin scaffold provides an opportunity to characterize side chain interactions between residues, which are separated by several positions in the sequence. Recent studies have emphasized the importance of aromatic clusters in stabilizing designed β-hairpins in aqueous solution (*35*, *36*, *42*). Peptides **2** and **4** possess Phe residues. In peptide **2**, the aromatic residues are placed at positions 2 and 6, which form the non-hydrogen-bonding position in the β-hairpin. The centroid to centroid distances (R_{cen}) of 5.37 Å for molecule A and 5.28 Å for molecule B are suggestive of favorable interactions between phenyl rings, which are oriented at an interplanar angle of 63° in molecule A and 47.5° in molecule B (Figure 4a). A similar close approach of Phe residues at facing positions across the β-hairpin has been observed in the crystal structure of Boc-Leu-Phe-Val-Aib-DAla-Leu-Phe-Val-OMe (*34*) and also in the -Leu-Phe-Val-DPro-Gly-Leu-Phe-Val-OMe segment of a 17-residue helix−hairpin peptide (*25*).

In the decapeptide **4**, Phe residues are placed at positions 3 and 10 on facing strands. Of the four molecules in the asymmetric unit, in two cases, molecules A and D, the Phe−Phe distances and the interplanar angles fall within the range suggested for productive aromatic interactions in proteins (*43*−*45*) (molecule A, $R_{cen} = 6.12$ Å and the interplanar angle = 86.98°; molecule D, $R_{cen} = 6.21$ Å and the interplanar angle = 88.28°; Figure 4b). In molecules B and C there is a rotation about the side chain torsion angle χ^1 for the two Phe residues, which places them much further apart (molecule B, $R_{cen} = 8.93$ Å; molecule C, $R_{cen} = 8.94$ Å).

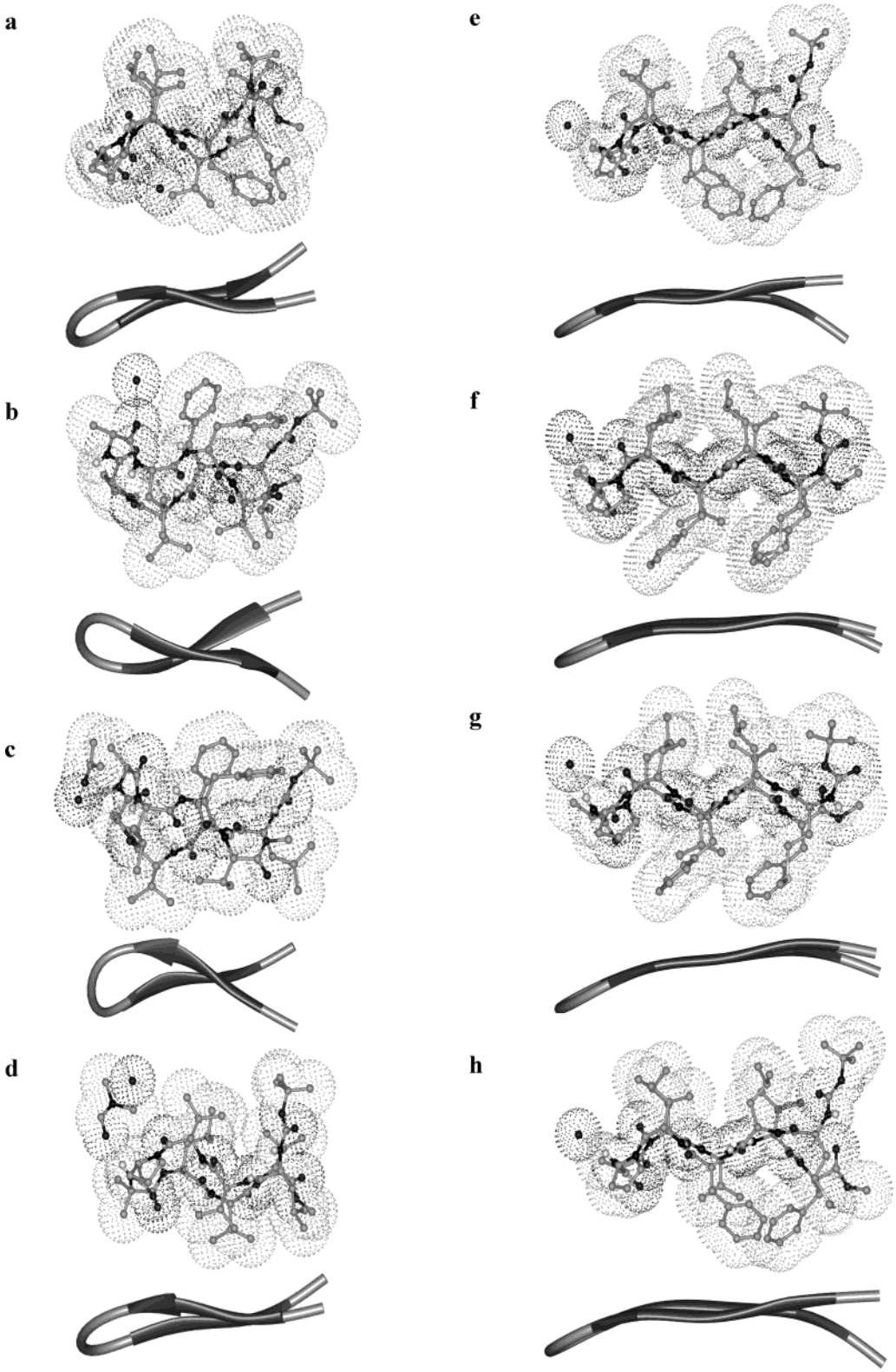

FIGURE 3: Side view of the molecules showing the pleated sheet in peptides **1**−**4**: (a) peptide **1**; (b and c) peptide **2**; (d) peptide **3**; (e−h) peptide **4**. The backbone fold is also shown schematically as a ribbon. Note the flattening of the sheet in **4**.

Peptide **2** also provides an interesting example of a possible aromatic−amide interaction involving a potentially favorable N−H···π interaction. In both molecules in the asymmetric unit of peptide **2**, the residue 1 NH group is not involved in any hydrogen-bonding interaction with an oxygen acceptor. As seen in Figure 4c, in both of the molecules in the asymmetric unit NH(1) approaches the Phe(7) aromatic ring with an NH···centroid distance of 4.65 Å and ∠NH··· centroid of 171.6° for molecule A. The values for molecule B are 4.81 Å and 155.5°. N−H···π interactions have been suggested to be potentially stabilizing elements in folded protein structures (*46*−*48*). Interestingly, in an ideal β-hairpin structure an O(8)···N(1) hydrogen bond should have formed. In peptide **2** molecule A, the C-terminal ester group is sandwiched between two aromatic rings, Phe(7) (intramolecular) and Phe(7) (intermolecular), from a symmetry-related

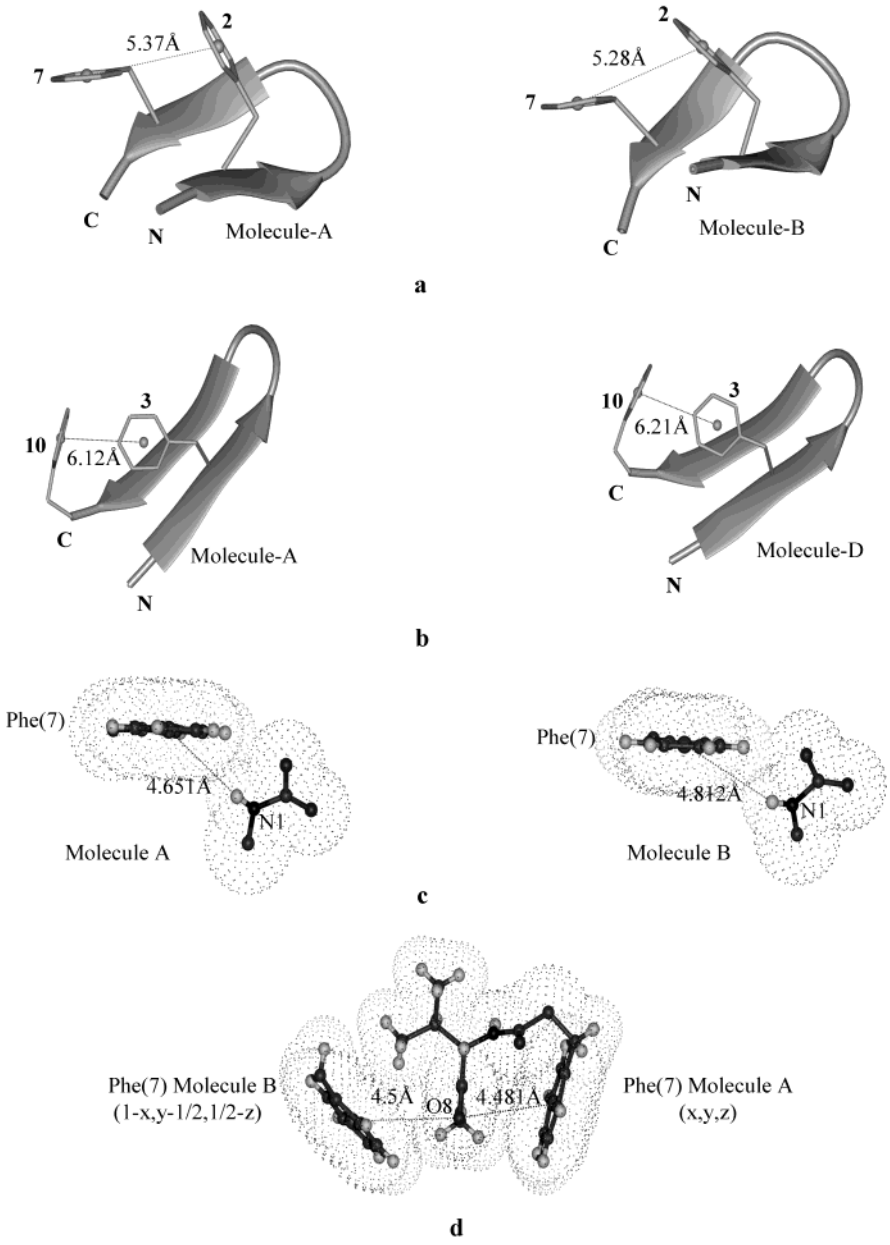

FIGURE 4: Aromatic−aromatic interaction between the Phe residues observed in peptide structures: (a) peptide **2**; (b) peptide **4**. (c) The backbone N−H$\cdots\pi$ interaction observed in peptide **2**. The distances between the centroids of the phenyl ring and the amide planes are indicated. The interplanar angles are 47.6° for molecule A and 51.6° for molecule B. (d) The oxygen aromatic ring interaction observed in peptide **2**. The ester carbonyl group lies perpendicular to the plane of the figure. The distances from the carbonyl oxygen to the centroids of the sandwiching phenyl rings are matched.

molecule B, resulting in an oxygen−aromatic ring interaction (Figure 4d) (*45*).

Packing of β-Hairpins in Crystals. As anticipated, a recurring mode of arrangement of peptide hairpins in crystals occurs by formation of a sheet-like hydrogen-bonding pattern between adjacent molecules. Figure 5 shows a view of the intermolecular interactions in peptide **1** as seen in a projection perpendicular to the plane of the sheet (down the *b*-axis). In an octapeptide hairpin an idealized structure would yield four intramolecular hydrogen bonds, leaving three free NH groups. Of these, the Xxx NH group is located in the turn region, with the central peptide unit oriented approximately perpendicular to the plane of the sheet. Inspection of the packing view in Figure 5 reveals that adjacent molecules are held together by intermolecular hydrogen bonds involving the exposed NH groups of 2 and 7. In addition, a third intermolecular hydrogen bond involving the residue 1 NH group is formed by distortion of the conformation of the N-terminal residue [Leu(1) $\psi = -55.4°$]. The CO group of residue 7 is thus involved in a bifurcated interaction with both NH(2) and NH(1) of an adjacent strand.

Figure 6 shows a view of the molecular packing in peptide **1**, a view down the *a*-direction, which is perpendicular to the view in Figure 5. The two-dimensional sheet is extended along the *c*-direction, with molecules in adjacent layers being related by a 2_1 screw operation which places the β-turn segments of adjacent layers in close proximity. The molecules are held together by bridging water molecules which hydrogen bond to the central peptide unit of the β-turn segment in the direction perpendicular to the plane of the sheet. Similar sheet formation involving an almost identical N-terminal distortion is observed in peptide **3** (Figure 7a).

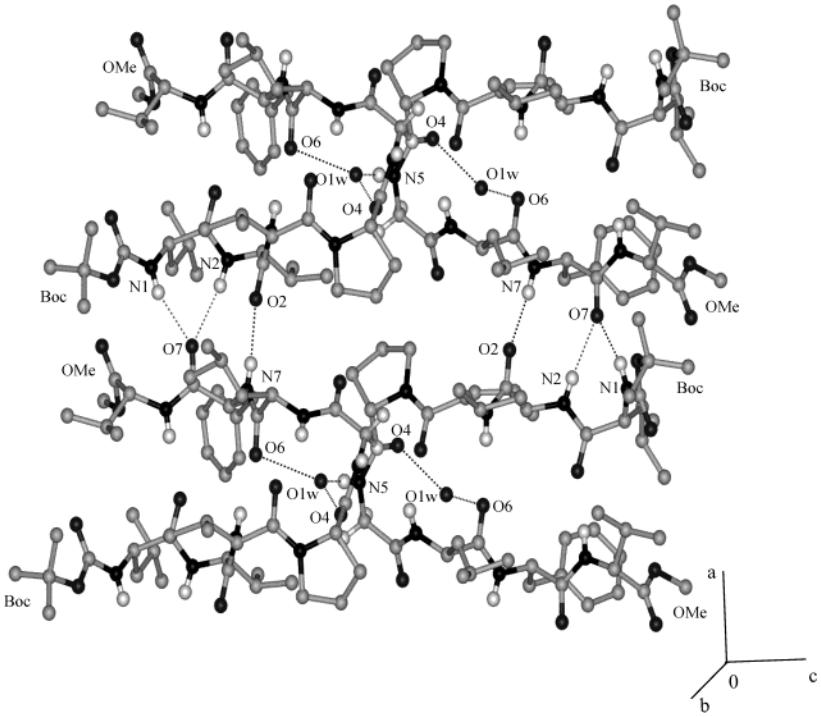

FIGURE 5: Individual extended β-sheets in crystals of peptide **1** formed by translation of molecules along the *a*-axis. The two layers of sheets are related by a 2_1 screw and are held by bridging water molecules in a perpendicular direction. Intramolecular hydrogen bonds are not shown.

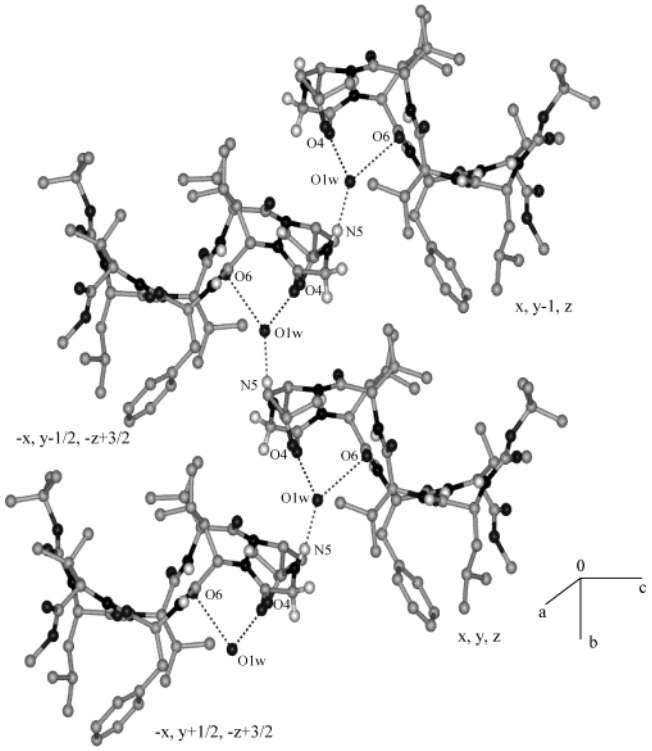

FIGURE 6: Side view of the β-hairpin packing in peptide **1** showing the water-mediated hydrogen bonds holding the symmetry-related molecules along the *b*-axis.

In the triclinic space group the hairpins are related only by translation. A lone dimethylformamide molecule forms a hydrogen bond to Aib(5) NH through its carbonyl group. Additional electron density, which may correspond to a water molecule, was also observed during the refinement. Interestingly, inclusion of water resulted in a drop in the crystallographic *R*-factor from 8.9% to 7.8%. The observed *B*-factor for the assigned water molecule (O1w) is 20.9 Å^2. This value may be compared to the *B*-factors for waters in the other hydrated octapeptide hairpins **1** and **2**, which lie between 8 and 15 Å^2. In the decapeptide **4**, of the four water molecules, two have *B* values of 12.4 and 12.8 Å^2, while the other two have higher values of 23.8 and 23.9 Å^2. Curiously, all non-hydrogen atoms lie at a distance greater than 4 Å from this assigned water molecule, which would imply that no hydrogen bonds are formed (Figure 7b).

Figure 8 shows a view perpendicular to that illustrated in Figure 7. In peptide **3**, hydrogen bond bridges mediated by solvents are not observed; rather the solvent appears to fill cavities in the structure. Packing in the direction perpendicular to the plane of the sheet is mediated primarily by the van der Waals interactions.

Decapeptide **4** contains two additional free NH groups, as compared to octapeptides **1**−**3**. The view of the packing shown in Figure 9 illustrates the formation of an almost ideal antiparallel β-sheet which runs through the crystal. Each molecule contains four intramolecular hydrogen bonds and forms four intermolecular hydrogen bonds to adjacent molecules on either side. Clearly, extension of the strands to provide additional hydrogen bond donors and acceptors facilitates ideal intermolecular sheet formation. The imperative of maintaining the registry of hydrogen bonds between molecules may contribute to the formation of a large asymmetric unit, containing as many as four independent molecules. The perpendicular view in Figure 10 illustrates bridging of the layer of sheets by water molecules, with the asymmetric unit containing four independent water molecules. The β-hairpins are packed in registered vertical columns with the projecting side chains providing a cluster of van der Waals interactions. In the β-turn region the corresponding segment of a hairpin of a neighboring column is inserted, such that a continuous network of bridging

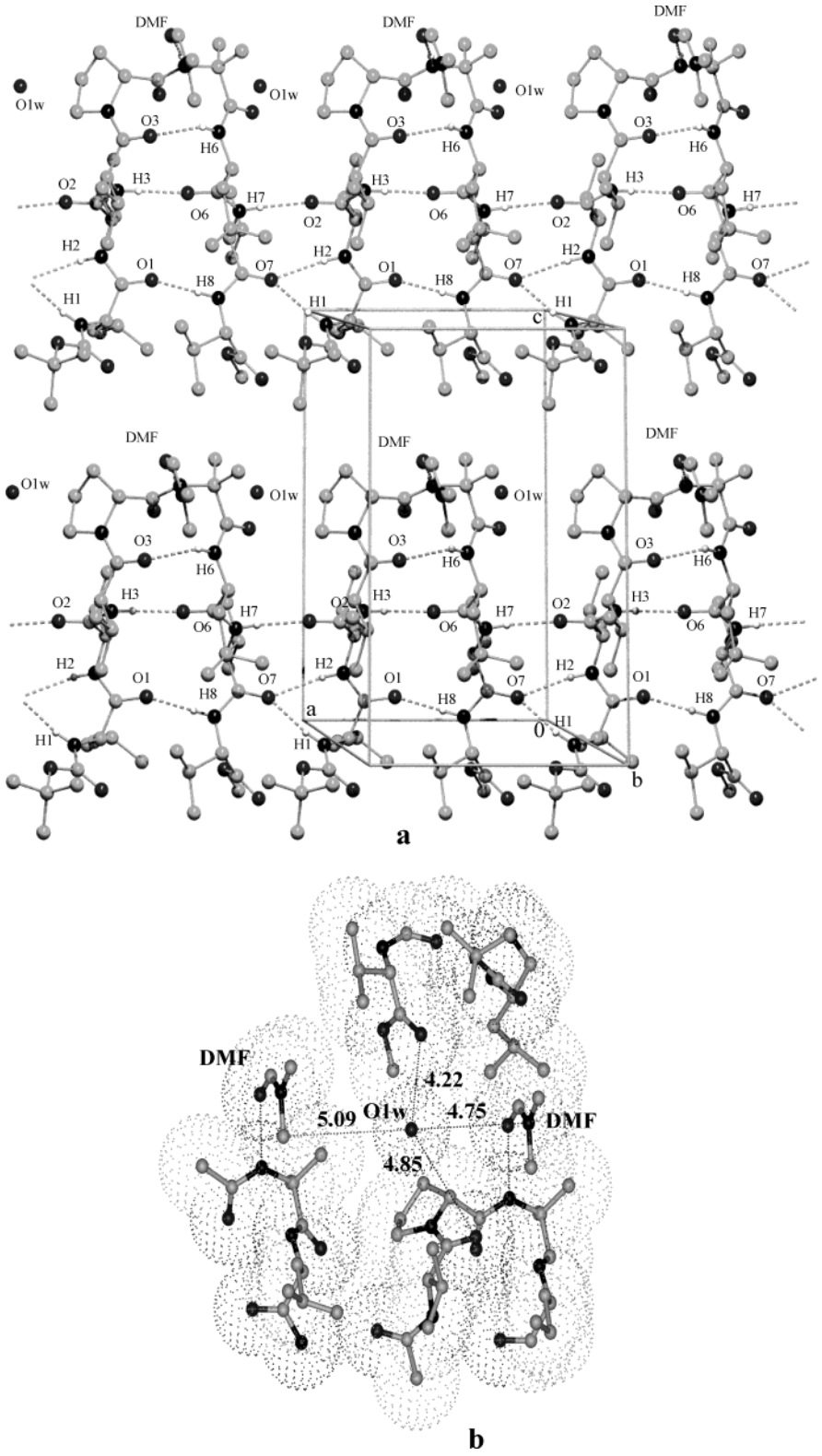

FIGURE 7: (a) Molecular packing of peptide **3** in crystals. (b) The solvent environment of the water molecule (O1w) and the closest distances of approach of non-hydrogen atoms are marked in angstroms. The van der Waals surfaces of the non-hydrogen atoms are shown.

hydrogen bonds is formed, involving the DPro-Ala peptide unit, which lies perpendicular to the hairpin plane. The van der Waals surfaces show the effectiveness of the packing in the direction perpendicular to the β-sheet. Figure 11 illustrates a view down the long axis of the hairpin in a direction approximately parallel to the strands. The effectiveness of side chain interactions in creating a continuous layer of β-sandwiches, piled upon one another, is clearly illustrated.

Peptide **2** reveals a more complex packing pattern in crystals. The asymmetric unit consists of two independent peptide hairpins along with three water molecules and one 2-propanol (Figure 12). Unlike the preceding structures, the two adjacent hairpins in the asymmetric unit do not lie parallel to one another; rather the hairpin planes are oriented at a large angle of approximately 67°. Two hydrogen bonds involving the NH and CO groups of Phe(2) hold the

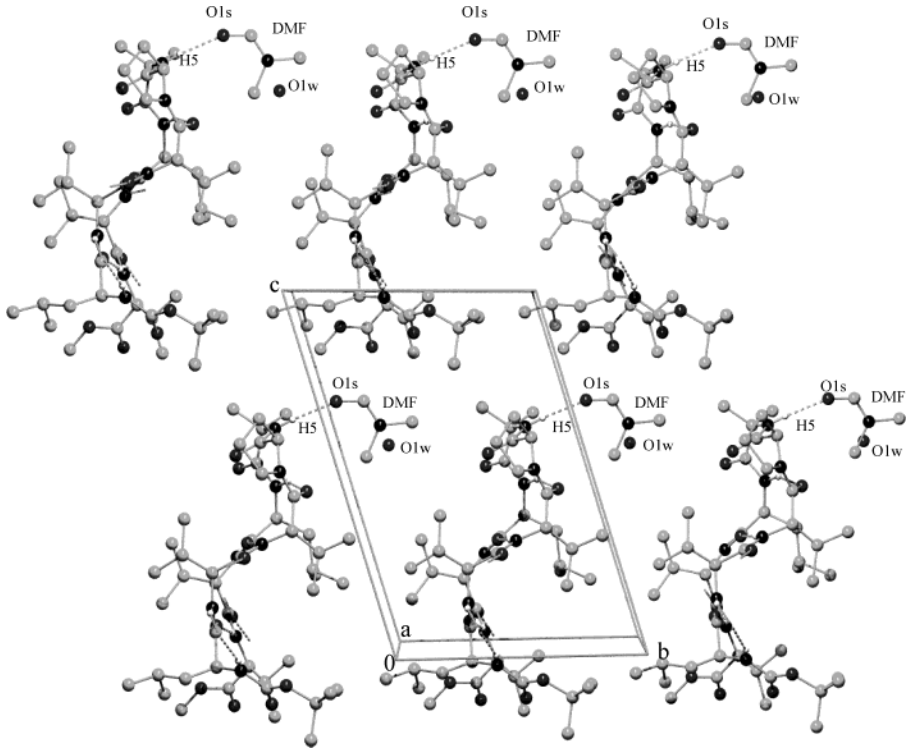

FIGURE 8: Side view of the molecular packing of peptide **3**.

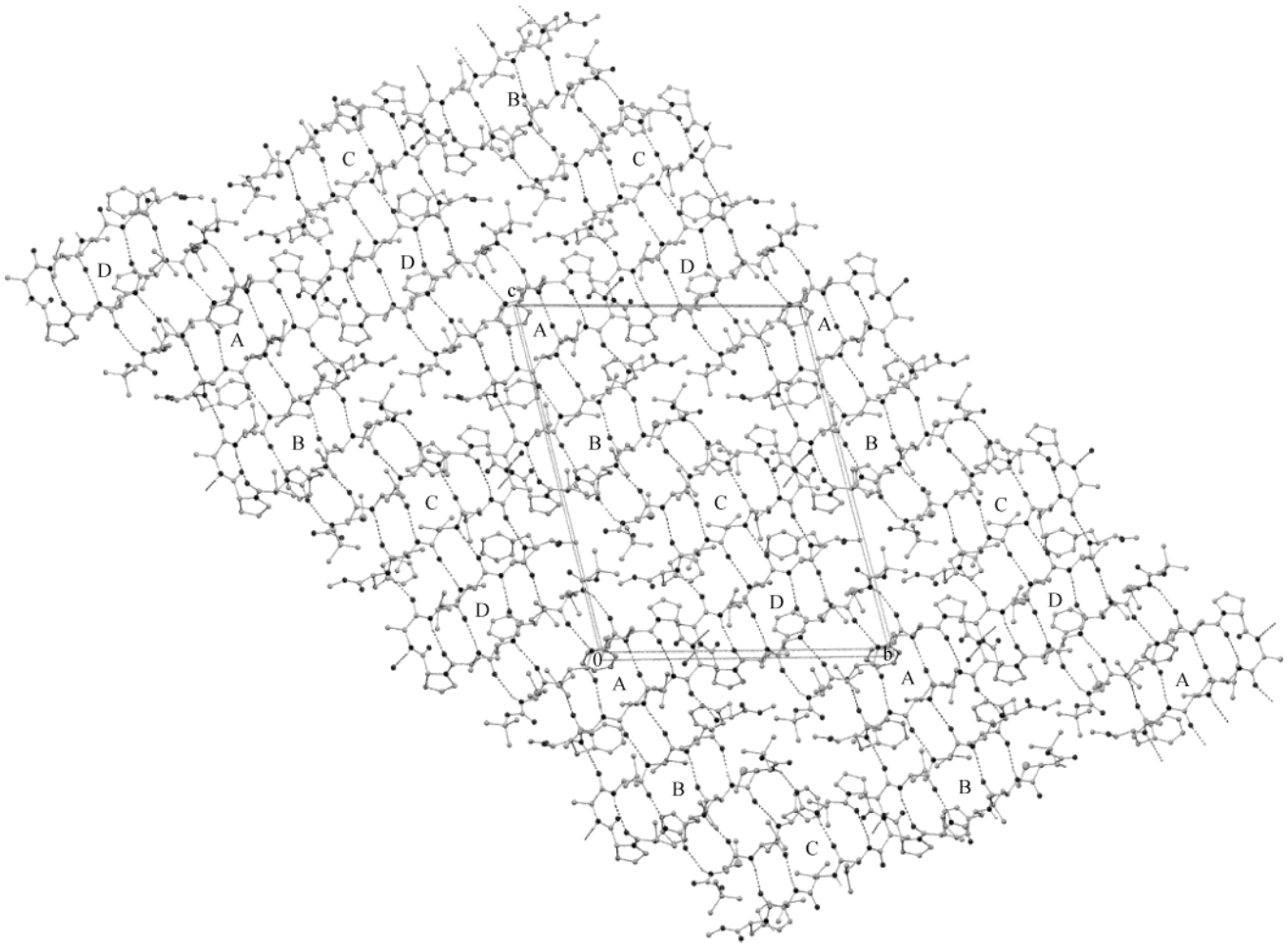

FIGURE 9: Molecular packing of the decapeptide **4** showing the infinite pleated sheet in crystals.

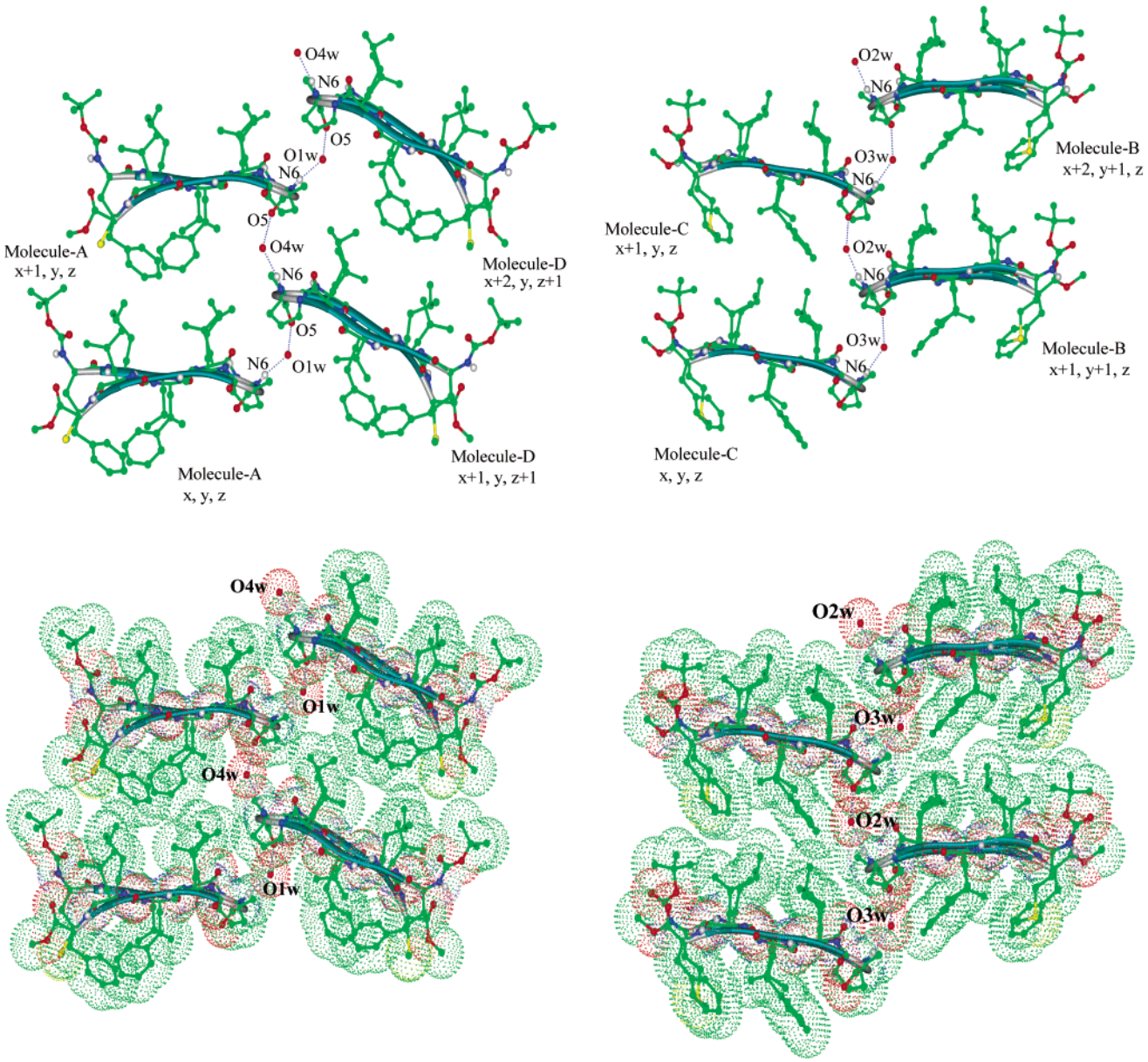

FIGURE 10: Side views of the molecular packing in crystals of peptide **4** showing the solvent-mediated hydrogen bond that binds the β-sheets into a supramolecular crystalline assembly. (Left) Water molecules O1w and O4w hold molecules A and D. (Right) Water molecules O2w and O3w hold molecules B and C in a direction perpendicular to the plane of the infinite β-sheet. The van der Waals surfaces of the non-hydrogen atoms are shown at the bottom.

molecules together. Extended packing of this asymmetric unit in the crystal is achieved through a complex intermolecular hydrogen-bonding pattern, involving two bridging water molecules O1w and O2w. (O2w is also involved in association of molecule A and its symmetry-related neighbors along the *b*-axis.) A third water molecule, O3w, forms hydrogen-bonded bridges along the *c*-direction between Ala(5) NH and Val(8) CO of symmetry-related B molecules (Figure 13). The lone 2-propanol molecule appears to fill cavities in the crystal and is hydrogen bonded only to O3w.

It is noteworthy that the structure of Boc-Leu-Val-Val-DPro-Gly-Leu-Phe-Val-OMe (**1**) determined in this study and conformer 2 of Boc-Leu-Val-Val-DPro-Gly-Leu-Val-Val-OMe determined earlier (*19*) are remarkably similar, both in molecular conformation and in the mode of association to form sheets. The isostructural nature of these two peptides suggests that the replacement of Val on one strand by an aromatic residue does not perturb local conformation or aggregation in a significant way. Comparison of Boc-Leu-Phe-Val-DPro-Ala-Leu-Phe-Val-OMe (**2**) determined in this study with peptide Boc-Leu-Val-Val-DPro-Ala-Leu-Val-Val-OMe reported earlier (*26*) reveals that the introduction of aromatic residues at the central position in strands results in a dramatically different packing arrangement. In the former, the two molecules in the asymmetric unit are arranged approximately orthogonal to one another, while a planar sheet arrangement is formed in the latter.

The hairpin structures presented in this report provide insights into β-sheet aggregation and packing into ordered arrays and may be relevant in considering models for amyloid formation. Fibril formation is an attribute of many polypeptide sequences and has been widely implicated in a variety of diseases (*49*). The β-sheet is a structural feature, which is common to all amyloid fibrils. The aggregation of β-strands to form insoluble fibrils involves packing of

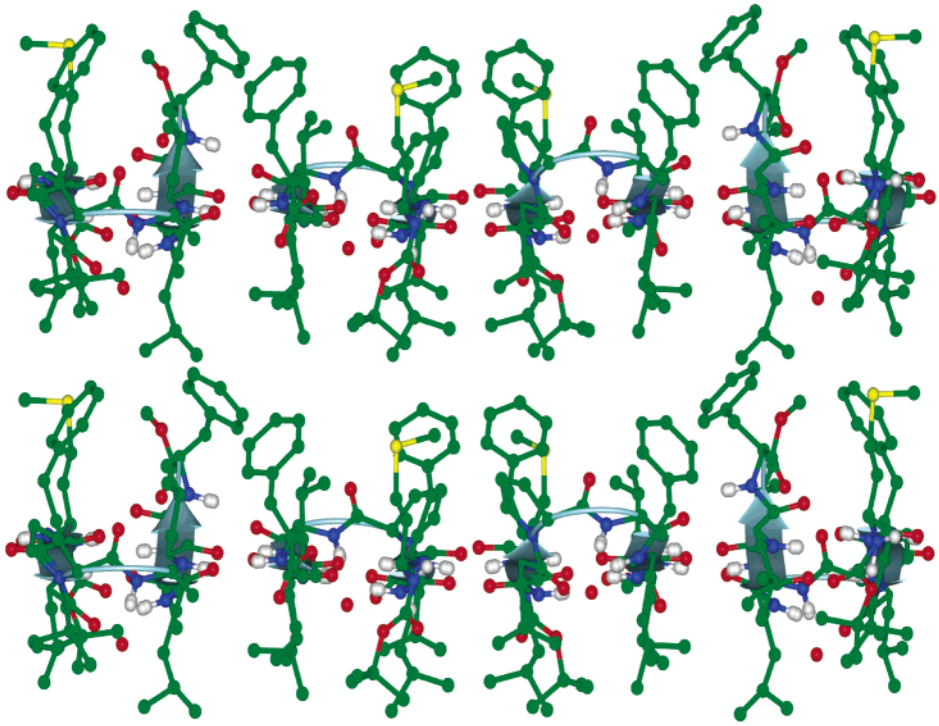

FIGURE 11: View down the long axis of the hairpin in peptide **4** in a direction approximately parallel to the strands.

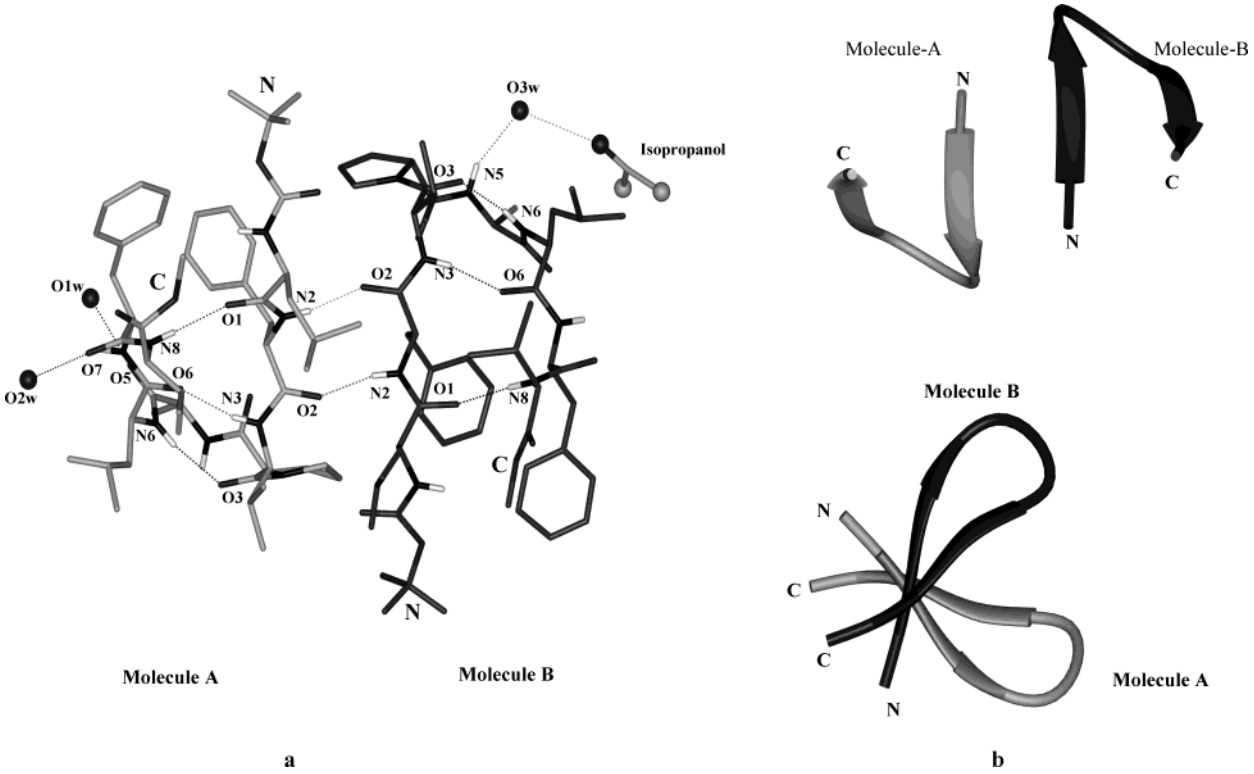

FIGURE 12: (a) The asymmetric unit of peptide **2**. All of the intra- and intermolecular hydrogen bonds in the asymmetric unit are shown as dotted lines. (b) The relative orientation of the two molecules in the asymmetric unit (top) viewed as in (a) and (bottom) viewed after a 90° rotation, shown in a ribbon representation.

β-strands in a direction approximately perpendicular to the plane of the β-sheet (*11*, *50*). β-Sheet formation appears to be a necessary condition for fibrillogenesis but is undoubtedly not a sufficient condition. Specific side chain interactions, which promote aggregation, must contribute to both the nucleation and stabilization of amyloids (*51*−*53*). Roles have been attributed to aromatic side chains (*54*). The structures of the peptide hairpins described in this report provide a wealth of detailed information on the packing of β-hairpins into crystalline lattices and the role of solvent in promoting specific aggregation. The structural information derived from this crystallographic analysis may have value in developing docking techniques which are currently being used in fibril modeling (*11*).

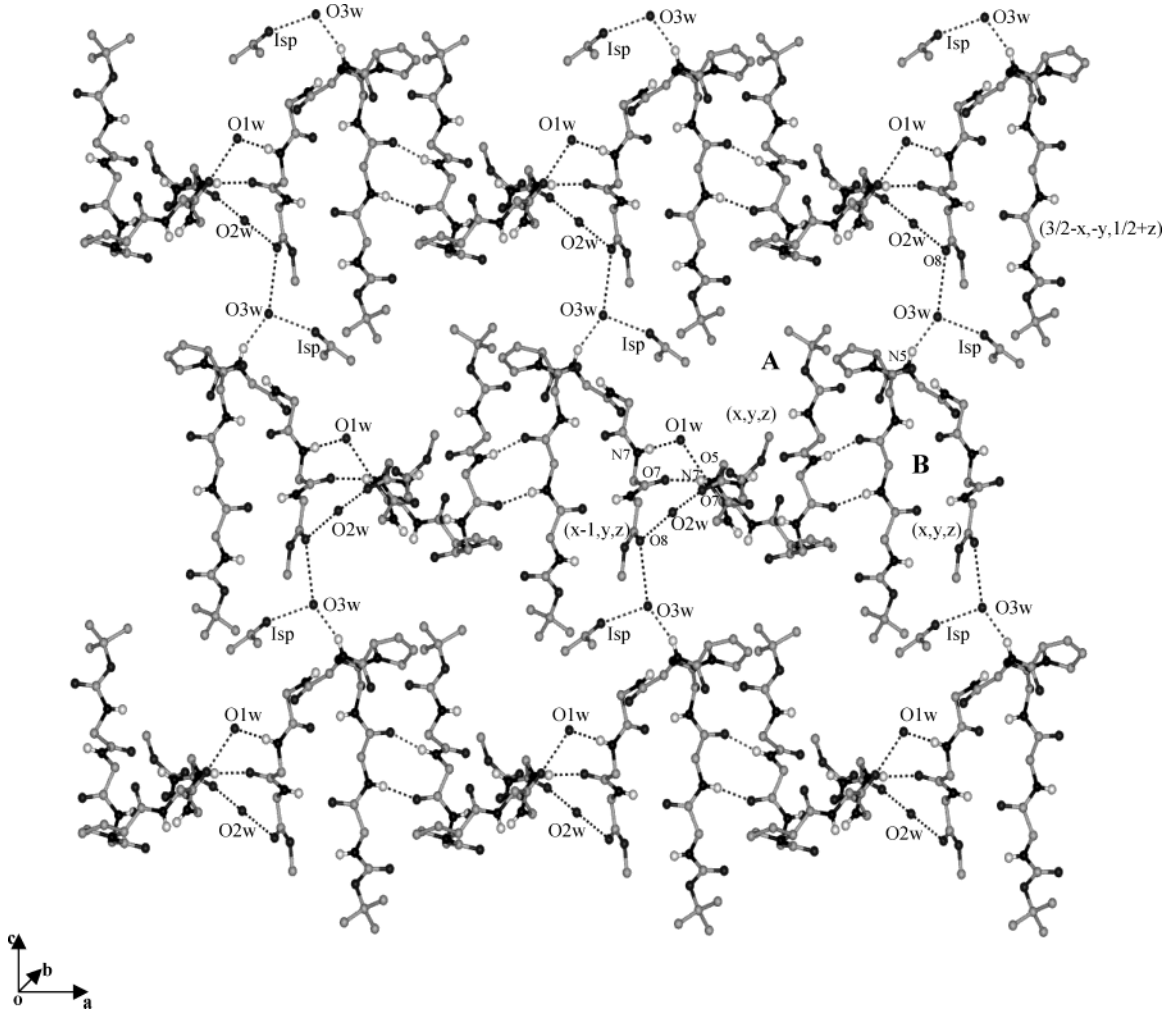

FIGURE 13: Molecular packing of peptide **2**. Only the intermolecular hydrogen bonds are shown. The side chain atoms are omitted for clarity.

CONCLUSIONS

The structures described in this report provide conformational and hydrogen-bonding information for eight independent β-hairpin peptides. The basic premise of the design strategy, which rests on the ability of DPro-Xxx segments to nucleate hairpin formation, is clearly established. The assembly of hairpins into crystals is achieved by sheet formation in two dimensions with hydrogen bond formation between the CO and NH groups that are directed outward from the hairpin. In the examples reported, intermolecular association in the sheets is predominantly between neighboring strands which run in antiparallel directions. Two distinct motifs can be discerned. When adjacent molecules are oriented in parallel fashion, intermolecular association brings the N-terminus of one molecule opposite to the C-terminus strand of a neighboring molecule, as exemplified in the structures of peptides **1** and **3**. In the case of peptide **4**, adjacent molecules are oriented in an antiparallel fashion, and the interhairpin association to form sheets is mediated by interaction between two antiparallel facing C-terminal or N-terminal strands. The assembly of β-sheet strips into a three-dimensional aggregate is mediated by side chain interactions and solvent bridges, in a direction approximately perpendicular to the plane of the sheets. In the β-turn segment, the central peptide unit (DPro-Xxx) is oriented such that the carbonyl and NH groups lie in a plane perpendicular to the sheet providing a locus for attracting solvent molecules, which can then bridge the hairpin structures in the third dimension. The crystalline octapeptide β-hairpins display appreciable buckling of the structure. The side chains of amino acid residues in the adjacent positions in the sequence project on opposite faces of the sheet, with side chain−side chain interactions further promoting the assembly in a direction perpendicular to the plane of the sheet. Cavities resulting from imperfect packing are filled by solvent molecules which do not always appear to be optimally hydrogen bonded. Notably, in the structure of peptide **3**, electron density corresponding to a water molecule is observed with no evidence for the close approach of any hydrogen bond donor or acceptor. The structure of peptide **2** reveals a more complex packing motif with adjacent hairpins lying approximately orthogonal to one another. The structures of the four peptide hairpins described in this report provide a basis for the design of structures optimized to promote intermolecular interactions suitable for assembly into single crystals. The crystalline state provides a definitive view of specific modes of molecular aggregation and assembly. A detailed understanding of packing motifs may also prove useful in developing models for the assembly of extended polypeptide strands into tangled sheets, which may result in the formation of insoluble materials often present in amyloid deposits and inclusion bodies.

ACKNOWLEDGMENT

We are grateful to G. M. Sheldrick (University of Göttingen, Germany) for kindly providing a copy of the program SHELXD. The CCD diffractometer facility was supported by the IRPHA program of the Department of Science and Technology, India.

REFERENCES

1. Salemme, F. R. (1983) *Prog. Biophys. Mol. Biol. 42*, 95−133.
2. Richardson, J. S. (1981) *Adv. Protein Chem. 34*, 167−339.
3. Schulz, G. E. (2000) *Curr. Opin. Struct. Biol. 4*, 443−447.
4. Sibanda, B. L., and Thornton, J. M. (1985) *Nature 316*, 170−174.
5. Sibanda, B. L., Blundell, T. L., and Thornton, J. M. (1989) *J. Mol. Biol. 206*, 759−777.
6. Hutchinson, E. G., and Thornton, J. M. (1994) *Protein Sci. 3*, 2207−2216.
7. Gunasekaran, K., Ramakrishnan, C., and Balaram, P. (1997) *Protein Eng. 10*, 1131−1141.
8. Wouters, M. A., and Curmi, P. M. (1995) *Proteins 2*, 119−131.
9. Gazit, E. (2002) *Curr. Med. Chem. 9*, 1667−1675.
10. Kelly, J. W. (1996) *Curr. Opin. Struct. Biol. 6*, 11−17.
11. Benyamini, H., Gunasekaran, K., Wolfson, H., and Nussinov, R. (2003) *J. Mol. Biol. 330*, 159−174.
12. Richardson, J. S., Richardson, D. C., Tweedy, N. B., Gernert, K. M., Quinn, T. P., Hecht, M. H., Erickson, B. W., Yan, Y., McClain, R. D., Donlan, M. E., and Surles, M. C. (1992) *Biophys. J. 63*, 1186−1209.
13. Lacroix, E., Kortemme, T., Lopez de la Paz, M., and Serrano, L. (1999) *Curr. Opin. Struct. Biol. 9*, 487.
14. Balaram, P. (1999) *J. Peptide Res. 54*, 195−199.
15. Venkatraman, J., Shankaramma, S. C., and Balaram, P. (2001) *Chem. Rev. 101*, 3131−3152.
16. Karle, I. L., and Balaram, P. (1990) *Biochemistry 29*, 6747−6756.
17. Kaul, R. K., and Balaram, P. (1999) *Bioorg. Med. Chem. 7*, 105−117.
18. Awasthi, S. K., Raghothama, S., and Balaram, P. (1995) *Biochem. Biophys. Res. Commun. 216*, 375−381.
19. Karle, I. L., Awasthi, S. K., and Balaram, P. (1996) *Proc. Natl. Acad. Sci. U.S.A. 93*, 8189−8193.
20. Haque, T. S., Little, J. C., and Gellman, S. H. (1996) *J. Am. Chem. Soc. 118*, 6975−6985.
21. Haque, T. S., and Gellman, S. H. (1997) *J. Am. Chem. Soc. 119*, 2303−2304.
22. Raghothama, S. R., Awasthi, S. K., and Balaram P. (1998) *J. Chem. Soc., Perkin Trans. 2*, 137−143.
23. Gellman, S. H. (1998) *Curr. Opin. Chem. Biol. 2*, 717−725.
24. Espinosa, J. F., and Gellman, S. H. (2000) *Angew. Chem., Int. Ed. 39*, 2330−2333.
25. Karle, I. L., Das, C., and Balaram, P. (2000) *Proc. Natl. Acad. Sci. U.S.A. 97*, 3034−3037.
26. Das, C., Naganagowda, G. A., Karle, I. L., and Balaram, P. (2001) *Biopolymers 58*, 335−346.
27. Karle, I. L., Gopi, H. N., and Balaram, P. (2001) *Proc. Natl. Acad. Sci. U.S.A. 98*, 3716−3719.
28. Gopi, H. N., Roy, R. S., Raghothama, S., Karle, I. L., and Balaram, P. (2002) *Helv. Chim. Acta 85*, 3313−3330.
29. Karle, I. L., Gopi, H. N., and Balaram, P. (2002) *Proc. Natl. Acad. Sci. U.S.A. 99*, 5160−5164.
30. Das, C., Raghothama, S., and Balaram, P. (1998) *J. Am. Chem. Soc. 120*, 5812−5813.
31. Das, C., and Balaram, P. (1999) *J. Chem. Soc., Chem. Commun.*, 967−968.
32. Venkatraman, J., Naganagowda, G. A., Sudha, R., and Balaram, P. (2001) *Chem. Commun.* 2660−2661.
33. Venkatraman, J., Naganagowda, G. A., and Balaram, P. (2002) *J. Am. Chem. Soc. 124*, 4987−4994.
34. Aravinda, S., Shamala, N., Rajkishore, R., Gopi, H. N., and Balaram, P. (2002) *Angew. Chem., Int. Ed. 41*, 3863−3865.
35. Tatko, C. D., and Waters, M. L. (2002) *J. Am. Chem. Soc. 124*, 9372−9373.
36. Waters, M. L. (2002) *Curr. Opin. Chem. Biol. 6*, 736−741.
37. Sheldrick, G. M. (1997) *SHELXS-97*, Program for the Crystal Structure Solution, Universität Göttingen, Germany.
38. Sheldrick, G. M. (1997) *SHELXL-97*, Program for the Refinement of Crystal Structures, Universität Göttingen, Germany.
39. Schneider, T. R., and Sheldrick, G. M. (2002) *Acta Crystallogr. D 58*, 1772−1779.
40. Venkatachalam, C. M. (1968) *Biopolymers 6*, 1425−1436.
41. Rose, G. D., Young W. B., and Gierasch L. M. (1983) *Nature 304*, 654−657.
42. Espinosa, J., Syud, F. A., and Gellman, S. H. (2002) *Protein Sci. 11*, 1492−1505.
43. Burley, S. K., and Petsko, G. A. (1985) *Science 229*, 23−28.
44. Singh, J., and Thornton, J. M. (1985) *FEBS Lett. 191*, 1−6.
45. Burley, S. K., and Petsko, G. A. (1988) *Adv. Protein Chem. 39*, 125−189.
46. Burley, S. K., and Petsko, G. A. (1986) *FEBS Lett. 203*, 139−143.
47. Mitchell, J. B. O., Nandi, C. L., McDonald, I. K., and Thornton, J. M. (1994) *J. Mol. Biol. 239*, 315−331.
48. Tóth, G., Watts, C. R., Murphy, R. E., and Lovas, S. (2001) *Proteins: Struct., Funct., Genet. 43*, 373−381.
49. Dobson, C. (1999) *Trends Biochem. Sci. 24*, 329−332.
50. Zanuy, D., and Nussinov, R. (2003) *J. Mol. Biol. 329*, 565−584.
51. Wang, W., and Hecht, M. H. (2002) *Proc. Natl. Acad. Sci. U.S.A. 99*, 2760−2765.
52. Broome, B. M., and Hecht, M. H. (2000) *J. Mol. Biol. 296*, 961−968.
53. López de la Paz, M., Goldie, K., Lacroix, E., Dobson, C. M., Hoenger, A., and Serrano, L. (2002) *Proc. Natl. Acad. Sci. U.S.A. 99*, 16052−16057.
54. Gazit, E. (2002) *FASEB J. 16*, 77−83.
55. IUPAC−IUB Commission on Biochemical Nomenclature (1970) *Biochemistry 9*, 3471−3479.

BI035522G